



## **Insight into aging behavior of superabsorbent polymer in cement-based materials to release microplastic pollution**

Downloaded from: <https://research.chalmers.se>, 2025-04-03 23:24 UTC

Citation for the original published paper (version of record):

Gu, L., Feng, J., Huang, L. et al (2025). Insight into aging behavior of superabsorbent polymer in cement-based materials to release microplastic pollution. *Case Studies in Construction Materials*, 22. <http://dx.doi.org/10.1016/j.cscm.2025.e04441>

N.B. When citing this work, cite the original published paper.



# Insight into aging behavior of superabsorbent polymer in cement-based materials to release microplastic pollution

Linan Gu<sup>a</sup>, Jingjing Feng<sup>a</sup>, Liming Huang<sup>b,\*</sup>, Zheyu Zhu<sup>c,\*</sup>

<sup>a</sup> College of Water Conservancy and Civil Engineering, Shandong Agricultural University, Taian, Shandong 271018, China

<sup>b</sup> Department of Architecture and Civil Engineering, Chalmers University of Technology, Gothenburg 41296, Sweden

<sup>c</sup> School of Materials Science and Engineering, Yancheng Institute of Technology, Yancheng, Jiangsu 224051, China

## ARTICLE INFO

### Keywords:

Aging behaviour  
Cement-based materials  
<sup>1</sup>H NMR  
Microplastic Pollution  
SAP

## ABSTRACT

Superabsorbent polymer (SAP) is widely used as an internal curing agent for cement-based materials. It is also a polymer that can potentially age over time, and the aging products may release microplastic pollution, but this has not been paid attention to. This work investigated the aging behaviour of SAP in both cement paste and simulated cement pore solution (CPS) for 70 d by the measurement of swelling ratio, particle size distribution, infrared spectroscopy, <sup>1</sup>H nuclear magnetic resonance, and thermogravimetric analysis. Results showed that the SAP in cement paste was aged, its ester groups decreased, carboxylate groups changed, and the aged SAP particle became difficult to re-swell. The molecular structure of SAP aged in CPS underwent significant alterations compared to the raw SAP and that aged in deionized water, with the ester groups nearly disappearing and carboxylate increasing significantly. SAP aged in CPS fragmented from 100–300 μm into smaller particle sizes ranging from 0.1 to 200 μm. Compared to the raw SAP, its mean value decreased by 38.3 %, and its swelling ratio decreased by 46.9 % when tested in CPS. The aged SAP particles were difficult to re-swell due to the formation of cross-linking between –COO<sup>-</sup> groups and cement hydration products through cations, such as Ca<sup>2+</sup>. The results indicate that the aging of SAP in cement-based materials is inevitable, and the aging products may release as potential microplastic pollution. Therefore, the aging behaviour of SAP cannot be ignored.

**Synopsis:** Superabsorbent polymer is a widely used agent in cement-based materials and also a potential aging polymer. Its aging products may leak into environmental systems and cause microplastic pollution. This study investigated the aging behavior of SAP and proposed that the aging of SAP in cement-based materials leads to the loss of internal curing and self-healing functions, with the aging product releasing microplastic pollution.

## 1. Introduction

Microplastic pollution has aroused great attention in recent years [1–3]. Some of them are plastic fragments (<5 mm in length [4, 5]) generated by the aging and disintegration of polymers such as polypropylene, polyurethane, polyacrylonitrile, polystyrene, polycarbonate, polyethylene, and polyester [6–8]. Most studies on microplastic pollution were focused on water ecosystems and soil environments, such as fishery activities [9,10] and agricultural plastics [11–13]. These microplastics can enter the human circulatory

\* Corresponding authors.

E-mail addresses: [limingh@chalmers.se](mailto:limingh@chalmers.se) (L. Huang), [17712937215@163.com](mailto:17712937215@163.com) (Z. Zhu).

<https://doi.org/10.1016/j.cscm.2025.e04441>

Received 23 September 2024; Received in revised form 7 February 2025; Accepted 21 February 2025

Available online 21 February 2025

2214-5095/© 2025 The Authors. Published by Elsevier Ltd. This is an open access article under the CC BY license (<http://creativecommons.org/licenses/by/4.0/>).

system directly through the food chain, contaminating drinking water and sea products [14–17], resulting in a serious threat to human health [18–20]. Furthermore, microplastics have even been detected in human blood vessels [21,22]. However, there are few reports on microplastic pollution caused by the potential release of organic substances in cement-based materials, such as internal curing agent [23–25], organic viscosity enhancing admixture and superplasticizer [26,27]. And these cement-based materials, such as water pipes and dams, may be in direct contact with drinking water, coastal, and groundwater environments.

Superabsorbent polymer (SAP) is a commonly used organic internal curing agent for cement-based materials [23–25]. It can adsorb water hundreds of times its weight, providing water absorption-release capabilities during cement hydration [23]. Thus it effectively mitigates the autogenous shrinkage of cement-based materials with a low water-to-cement ratio (w/c) [24]. This can be attributed to its special molecular structure. Firstly, it is a macromolecular compound and its molecular chain contains polymerized acrylates to form macromolecules with strong hydrophilic functional groups such as carboxyl ( $-\text{COO}^-$ ), hydroxyl ( $-\text{OH}$ ), and a large number of ionizable cations that can be ionized in water [28–30]. Secondly, repulsive forces between groups with the same polarity cause SAP to expand after water absorption [29,30]. In a solution environment, SAP particles expand and form three-dimensional networks with

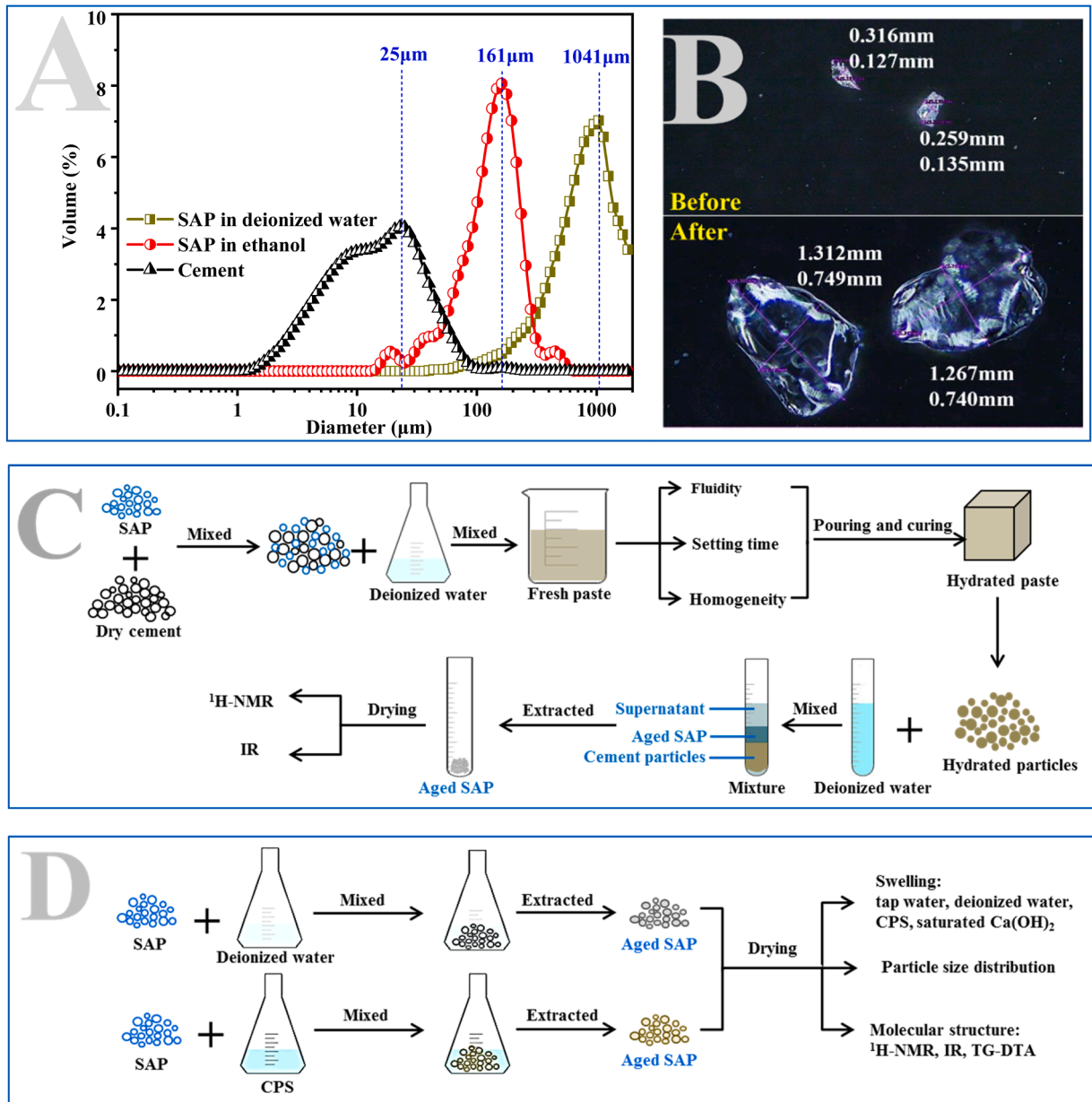


**Fig. 1.** Materials and sample preparation (A: Particle size distribution, B: SAP particles before and after swelling, C: Aged SAP in cement paste, D: Procedure of the experiment for testing the aging behavior of SAP in CPS).

low crosslinking to achieve high water absorption [25,30]. The lower the crosslinking degree, the higher the pore size of the crosslinking network, and the higher the water absorption ratio [30,31]. Thus, SAP can store a significant amount of water and gradually release it to mitigate autogenous shrinkage as an organic internal curing agent in cement-based materials [23–25]. In addition, it can also serve as a self-healing additive of cracks due to the uptake of water penetrating a crack in concrete [32,33].

Meanwhile, SAP is a macromolecular polymer that has the potential to degrade over time. In other fields, Ai et al. [30] reported that the SAP degraded gradually after 35 d in the soil, and its water retention effect had been greatly reduced according to field measurements. In the field of cement-based materials, it was also found that  $\text{Ca}^{2+}$  ion was trapped within the SAP polymer, resulting in a reduction in the swelling after water absorption [24]. Meanwhile, some SAP were split when a crack occurred but it was still bonded to the cement matrix [32]. However, it remains uncertain whether SAP ultimately ages in cement-based materials and whether the aged SAP would still be capable of effectively reabsorbing water. This could lead to a decrease or even a complete loss of its internal curing and self-healing effects. Furthermore, its degradation may accelerate as the service life of the concrete structure prolongs, leading to the release of microplastic pollution. Considering that multitudinous concrete structures, such as water pipes and dams, are in direct contact with drinking water and coastal areas, the potential microplastic pollution caused by aged SAP leaked from cement-based materials cannot be ignored. It may pose a risk to the safety of the surrounding water environment and human health.

Previous research on SAP in cement-based materials mainly focused on its internal curing function. However, research is lacking on SAP aging behavior in such materials, the re-swelling ability of aged SAP, and the potential microplastic pollution risks posed by aging products. Thus, the SAP in cement paste after 70 d of curing was extracted, and then the molecular structure was analyzed using methods such as infrared spectroscopy (IR),  $^1\text{H}$  nuclear magnetic resonance ( $^1\text{H}$  NMR) and thermogravimetric analysis (TG). Meanwhile, various simulated cement pore solutions (CPS) were developed in this work to minimize errors caused by soluble materials derived from cement paste. Then, the aging behavior of SAP in CPS was investigated over a period of 70 d to provide a reference for exploring the mechanisms of aging in cement-based materials and the possible release of microplastic pollution.

## 2. Materials and methods

### 2.1. Materials

In this paper, P•I 42.5 Portland cement with a specific surface area of  $340\text{ m}^2/\text{kg}$  was offered by China United cement Co., Ltd. The commercial SAP, a sodium acrylate type of polymer, supplied by Weng Jiang Chemical Reagent Co., Ltd was chosen in this work. The particle size distribution of SAP and cement is shown in Fig. 1A. The morphology of SAP particles before and after swelling is shown in Fig. 1B. To compare the aged SAP obtained from cement paste with the aged SAP from CPS, the deionized water was used as the mixing water.

### 2.2. Sample preparation

To explore the aging behavior of SAP in cement-based materials, the SAP was extracted from cement paste after 70 d curing, as shown in Fig. 1C. First, the SAP content used in casting paste was determined based on fluidity, setting times, and homogeneity. Cement and SAP particles were mixed before adding water. Subsequently, the cement paste was mixed with water and then cured for 70 d. In this part, the w/c was 0.5, the SAP content was 0.0 %, 0.1 %, 0.4 %, and 1.0 % by mass of cement, and the test ambient temperature was  $23 \pm 2\text{ }^\circ\text{C}$ . Afterwards, the aged SAP particles were extracted mainly based on a previous report [25]. Then, the SAP particles were washed five times with deionized water and ethanol, and dried in a vacuum at  $40 \pm 2\text{ }^\circ\text{C}$  for 48 h before conducting the IR and  $^1\text{H}$  NMR tests.

Fig. 1D shows the schematic representation of the sample preparation and testing process for studying the aging behavior of SAP in solutions. It was also found that  $\text{Ca}^{2+}$  ions was trapped within the SAP polymer, resulting in a reduction in the swelling after water absorption [24]. Based on this, we designed three simulated solutions with varying concentrations of  $\text{Ca}^{2+}$  ions, the deionized water (DW), simulated cement pore solution (CPS: NaOH 0.10 mol/L, KOH 0.32 mol/L,  $\text{Ca}(\text{OH})_2$  0.01 mol/L), and saturated  $\text{Ca}(\text{OH})_2$  (CH) solution, which correspond to  $\text{Ca}^{2+}$  concentrations of 0, 0.01, and 0.02 mol/L, respectively. Firstly, SAP particles were added to DW, CPS and saturated CH, respectively. After being placed at  $23 \pm 2\text{ }^\circ\text{C}$  for 70 d, SAP was washed five times with deionized water and ethanol to eliminate soluble impurities. Subsequently, the sample was dried in a vacuum at  $40 \pm 2\text{ }^\circ\text{C}$  for 48 h before the tests. However, it was worth noting that the aged SAP in saturated  $\text{Ca}(\text{OH})_2$  solution for 70 d was hardly able to absorb water again to achieve re-swelling. Therefore, the properties of extracted SAP, including those aged in deionized water (A-DW) and aging in CPS (A-CPS), were assessed through the swelling ratio test, particle size distribution measurement, TG, IR, and  $^1\text{H}$  NMR.

### 2.3. Homogeneity of SAP in cement paste

It is crucial to determine the optimal SAP content in the study of extracting aged SAP from cement paste. Thus, the homogeneity of SAP at 0.0 %, 0.1 %, 0.4 %, and 1.0 % contents in paste was determined based on setting times, fluidity, and distribution [34,35]. Setting times of paste were tested according to the Chinese national standard GB/T1346–2011 [36] using a Vicat Apparatus and a w/c of 0.254. The fluidity of pastes was measured with a w/c of 0.5 according to the Chinese national standard GB/T8077–2000 [37]. Then, the homogeneity of SAP in cement paste was observed using a light microscope. The pastes were prepared with a w/c of 0.5, and then poured into a  $2 \times 2 \times 2\text{ cm}^3$  mold. After 24 h, they were demolded and then cured at  $23 \pm 2\text{ }^\circ\text{C}$  for 7 d. Subsequently, the internal morphology and distribution of SAP in cement pastes were observed.

## 2.4. IR spectrum

To explore the aging behavior of SAP in cement-based materials, we recorded IR spectra of raw SAP and SAP extracted from cement paste and aged in various solutions to analyze its molecular structure changes before and after aging. The IR spectroscopy was performed on an EQUINOX 55 (Bruker) spectrometer. The raw SAP and aged SAP particles were washed five times with deionized water and ethanol to remove soluble impurities. Then, the samples were dried in a vacuum at  $40 \pm 2$  °C for 48 h, and finally ground into powder for the IR tests. The frequency range was  $400\text{--}4000$   $\text{cm}^{-1}$  with  $4.0$   $\text{cm}^{-1}$  resolution and the samples were scanned 64 times.

## 2.5. $^1\text{H}$ NMR spectrum

$^1\text{H}$  NMR was also used to study the molecular structure changes of SAP during aging in cement-based materials. The  $^1\text{H}$  NMR spectra of raw SAP and the SAP extracted from cement paste and aged in various solutions (extraction method in Section 2.4) were recorded to analyze structure alterations. The samples were ground into powder, and 0.10 g of the powder was mixed with 0.55 ml of deuterium oxide ( $\text{D}_2\text{O}$ ). The  $^1\text{H}$  NMR in  $\text{D}_2\text{O}$  was performed on a Bruker 400 M nuclear magnetic resonance analyzer and the samples were scanned 64 times at  $23 \pm 2$  °C.

## 2.6. Swelling

The swelling properties of SAP before and after aging were tested using the tea-bag method [24,31,39] to investigate whether aged SAP will still be capable of reabsorbing water effectively. Dry SAP particles ( $m_1$ ) about 1.00 g were placed at the bottom of the tea-bag ( $m_2$ ), which had been pre-wetted with the testing solvents, including deionized water, tap water, CPS and  $\text{Ca}(\text{OH})_2$  saturated solution. The tea-bag containing SAP was soaked into the different testing solvents for 1 h, and then the swollen tea-bag was suspended in the air for 10 min. Finally, the tea-bag was weighed ( $m_3$ ). The swelling ratio ( $Q$ ) can be calculated according to Eq. (1). At least three individuals within one batch of tea-bags and test solvent were performed.

$$Q = \frac{m_3 - m_2 - m_1}{m_1} \quad (1)$$

## 2.7. Particle size distribution

To further investigate whether aged SAP splits and whether the size of its degraded fragments poses a potential risk for microplastic pollution, the particle size distribution of raw SAP and aged SAP was analyzed. The particle size distribution of SAP particles was measured by a LS230 laser diffraction particle size analyzer. In the test of raw materials, deionized water and alcohol were used as dispersion media, and only alcohol was used as a dispersant in the particle size test of the SAP aged in solution.

## 2.8. TG analysis

The thermal decomposition process in polymers is closely related to their molecular structure [31]. To further investigate the mechanisms of changes in SAP's swelling properties and particle size, TG analysis was performed on raw and aged SAP (extracted following Section 2.4). This aimed to study the thermal decomposition and molecular structure evolution of the SAP. The TG was measured by a Netzsch STA 409 thermal analyzer at an atmosphere of oxygen-free nitrogen. The testing temperature range was  $30\text{--}900$  °C with a heating rate of  $10$  °C/min.

# 3. Results and discussion

## 3.1. Aging behavior of SAP in cement paste

To investigate the aging behavior of SAP in cement paste, the appropriate SAP content was determined for the paste. The optimal dosage of SAP varies although many scholars have explored its role in cement. It was reported that 0.5–1.0 % [25] can store and release the absorbed water to provide the internal curing performance. 1.0 % SAP effectively sealed cracks in cementitious materials and resulted in a reduction of water runoff per unit time by 52–72 % [32]. Liu et al. [33] also found that 28.4 wt% SAP can facilitate the plugging of microcracks through percolation theory. But more SAP results in a less homogeneous cement paste. In this study, the setting times and fluidity of cement paste mixed 0.0 %, 0.1 %, 0.4 %, and 1.0 % SAP were tested, and the homogeneity of SAP in the hardened paste was observed. Furthermore, the molecular structure of SAP extracted from paste was also tested using IR spectra and  $^1\text{H}$  NMR spectra.

### 3.1.1. Homogeneity of SAP in cement paste

Fig. 2A and B display the setting times and fluidity of cement paste with various contents of SAP. On the whole, the setting times and fluidity decrease with the increase of SAP content, and the setting times comply with the Chinese national standard GB175–2020 [38]. The initial and final setting times of the 1.0 % SAP group were reduced by 52 min and 33 min, respectively, compared with the control. The addition of 1.0 % SAP reduced the fluidity of paste from 224 mm to 202 mm. SAP absorbs some of the water in fresh paste,

which results in a reduction of free water. Consequently, this leads to a reduction in the effective w/c for pastes, so the addition of SAP (< 1 %) shortens the setting times and reduces the fluidity of cement paste.

Fig. 2C exhibits the diagram of the SAP distribution in cement paste. The apparent porosity of cement-based materials can be directly observed [40]. In the control group, there are circular pores with a diameter of 0.5–2.0 mm in the paste, resulting from air bubbles. In the pastes with SAP, there are also smaller pores, and their shape is more closely related to the shape of SAP particles. These characteristics can help to distinguish between pores formed by SAP particles and air bubbles. The SAP particles are evenly distributed, and the particle diameter is about 0.20–0.25 mm in the 0.1 % SAP group. However, a very poor uniformity of particle distribution and increased number of air bubbles are observed in the paste with the 0.4 % and 1.0 % SAP. Based on the above results, the 1.0 % SAP group was selected for further investigation of the aging behavior of SAP in cement paste.

### 3.1.2. IR spectra of SAP before and after aging in cement paste

To further explore the aging behavior of SAP in cement paste, IR spectra of raw SAP and SAP extracted from cement paste were recorded to analyze the change of their molecular structure. The SAP used in this work is a synthetic sodium acrylate polymer. As shown in Fig. 3A, in the IR spectrum of raw SAP, the bands at  $3590\text{ cm}^{-1}$  and  $3280\text{ cm}^{-1}$  correspond to the O–H bond in free water and bound water, respectively [31,41,42]. Peaks around  $1720\text{ cm}^{-1}$  and  $1115\text{ cm}^{-1}$  are related to the stretching vibration of the C=O bond [29] and the C–O bond [43] in the ester group (–COOC–), respectively, indicating the existence of the ester group. The strong bands around  $1573\text{ cm}^{-1}$  and  $1408\text{ cm}^{-1}$  are considered to be related to the carboxylate group (–COO–) [31,44,45]. The peak at  $870\text{ cm}^{-1}$  is related to the out-of-plane bending vibration of the C–H bond of unsaturated olefins (–CH=CH<sub>2</sub>–) in the SAP molecule [46].

However, Fig. 3A also shows that the IR spectrum of SAP extracted from cement paste is different from that of raw SAP. The O–H bonds emerge into one wide peak at around  $3425\text{ cm}^{-1}$ , and their intensity is increased compared to the raw SAP, implying more free water and bound water were generated in the SAP extracted from cement paste. Peaks at  $1720\text{ cm}^{-1}$  and  $1115\text{ cm}^{-1}$  are significantly reduced, indicating the reduction in the –COOC– group [29,43] and the reduction in the degree of crosslinking in aged SAP. Specifically, the peak at  $1573\text{ cm}^{-1}$  related to –COO– group [31,44,45] decreases and shifts to  $1673\text{ cm}^{-1}$ , while the peak at  $1408\text{ cm}^{-1}$  increases and shifts to  $1420\text{ cm}^{-1}$ . This suggests that the types of carboxylate groups may change during the aging process of SAP in cement paste. In addition, the new peaks appearing around  $968\text{ cm}^{-1}$  and  $874\text{ cm}^{-1}$  may be related to the C–H bond vibration of –CH=CH<sub>2</sub>– [46] in the aged SAP molecule. More unsaturated olefins may be formed due to the fracture and aging degradation of SAP molecular chains.

### 3.1.3. <sup>1</sup>H NMR spectra of SAP before and after aging in cement paste

To further explore the evolution of the molecular structure of SAP during the aging process in cement, the <sup>1</sup>H NMR spectra of raw

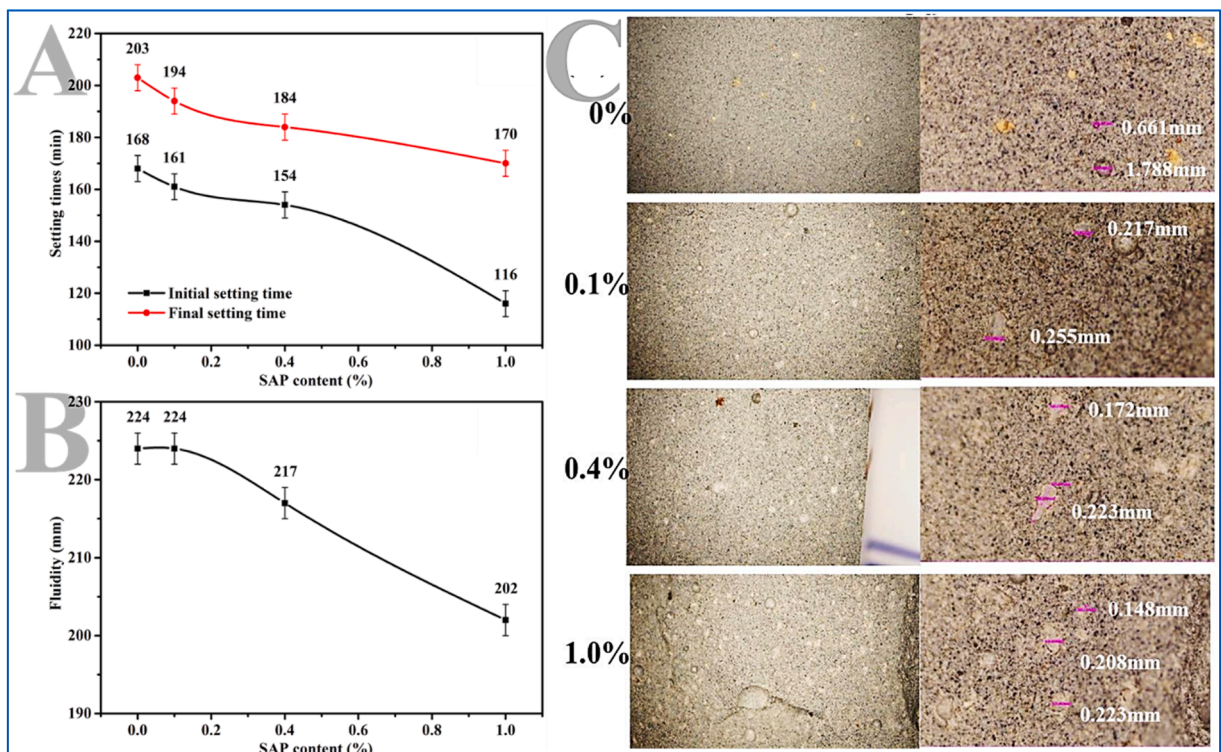


Fig. 2. Homogeneity of paste mixed SAP (A: Setting times, B: Fluidity C: Distribution of SAP in paste).

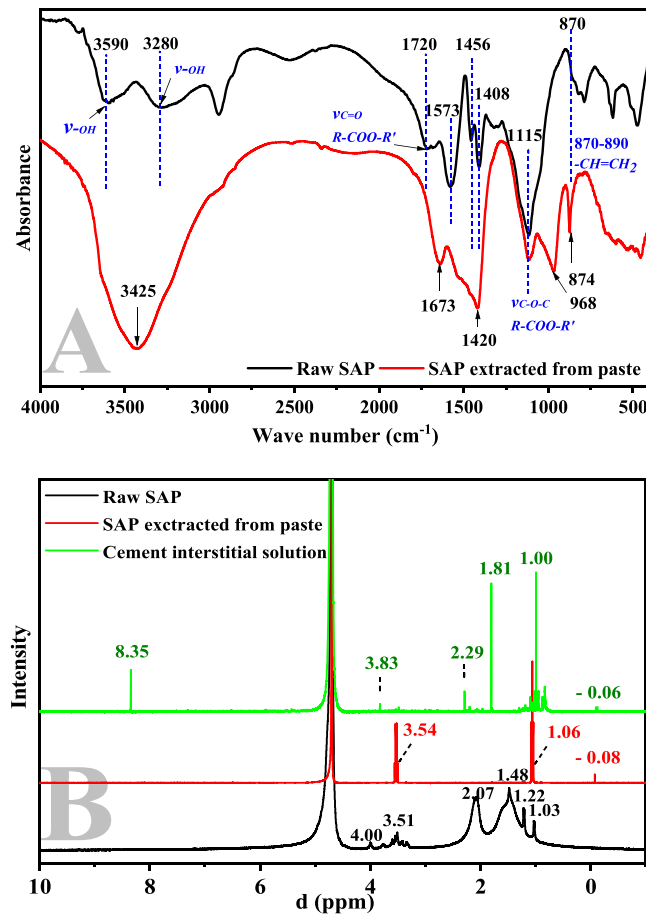


Fig. 3. IR and  $^1\text{H}$  NMR spectrum of raw SAP and SAP extracted from paste (A: IR, B:  $^1\text{H}$  NMR).

SAP and SAP extracted from cement paste were measured, and the results are presented in Fig. 3B. The raw SAP is a macromolecular compound, and its chemical shift at 1.03 ppm is related to incompletely polymerized  $-\text{CH}_3$  groups [47]. The peak around 1.22–1.48 ppm is due to the  $-\text{CH}_2-$  linked to the carboxylate ( $-\text{CH}_2-\text{CH}-\text{COO}^-$ ) [47,48]. And the multiple peaks in this region are associated with the incomplete polymerization of sodium acrylate polymers with different molecular weights in commercial SAP. Peaks at chemical shift around 2.07 ppm and 3.51 ppm are derived from the  $-\text{CH}-$  directly connected to the carboxylate ( $-\text{CH}-\text{COO}^-$ ) [47,48] and  $-\text{CH}$  in the end alcohol [29], respectively. The peak at 4.00 ppm may be associated with ester-linked alcohol or carboxyl-linked alcohol ( $-\text{O}-\text{H}$ ) [29] in SAP molecule.

Fig. 3B also displays the  $^1\text{H}$  NMR spectra of the SAP extracted from cement paste, and the cement interstitial pore solution was also tested to minimize the effects of soluble materials. In aged SAP, three peaks appear at approximately  $-0.08$ ,  $1.06$ , and  $3.54$  ppm. This pattern differs from that of raw SAP but is similar to the  $^1\text{H}$  NMR spectrum of cement interstitial pore solution. Chemical shift around  $3.54$  ppm may indicate the presence of  $-\text{CH}-$  in the end alcohol [29]. This result implies a significant change in the molecular structure of SAP extracted from cement paste. It is challenging for aged SAP particles to re-absorb  $\text{D}_2\text{O}$  solvent, which makes it difficult to detect the presence of  $^1\text{H}$  in the molecular structure of aged SAP. The reduction swelling ratio in SAP occurred when a large quantity of  $\text{Ca}^{2+}$  is trapped within the SAP polymer [24]. In a solution environment, the  $-\text{COO}^-$  groups in raw SAP become ionized while cement hydration products such as  $\text{Ca}^{2+}$  are generated. These  $\text{Ca}^{2+}$  ions may enter the SAP particles and cross-link with  $-\text{COO}^-$  groups. The chemical bond with  $\text{Ca}^{2+}$  leads to an increment in the cross-linker density and the contraction of the SAP network. As a result, additional uptake of the  $\text{D}_2\text{O}$  solvent is blocked, causing a reduction in the re-swelling of SAP.

The IR and  $^1\text{H}$  NMR results above indicate that, after 70 d in cement paste, the SAP particles aged. The ester group decreased, while the carboxylate group undergoes changed, converting into different types of aging products. Consequently, the aged SAP particles were difficult to re-swell and absorb water.

### 3.2. Aging behavior of SAP in solutions

To minimize errors caused by soluble materials derived from cement paste, various simulated cement pore solutions were prepared

in this study, including deionized water and CPS. Afterward, the aged SAP in the simulated cement pore solutions was obtained after 70 d. Subsequently, their swelling properties and particle size were evaluated, and their molecular structures before and after aging were investigated by TG, IR, and  $^1\text{H}$  NMR.

### 3.2.1. Swelling property of the SAP aged in solution

To investigate whether aged SAP would still be capable of effectively reabsorbing water, we tested the swelling property of SAP before and after aging in the deionized water, tap water, CPS, and a saturated  $\text{Ca}(\text{OH})_2$  solution, and the results are presented in Fig. 4. As shown in Fig. 4, the swelling ratio of raw SAP in deionized water, tap water, CPS, and saturated  $\text{Ca}(\text{OH})_2$  is 179.6, 102.8, 33.7, and 49.1 g/g, respectively. Overall, the swelling ratio of raw SAP decreases with the increase of ion concentration in testing solvents. Meanwhile, the A-CPS group and A-DW group almost presented a similar tendency as the raw SAP. This is because the higher ion concentration induces a lower water absorption in raw SAP [31,49].

Fig. 4 also shows that the swelling ratio of the A-DW group in all solvents is lower than that of raw SAP. Although SAP was considered to be a chemically stable plastic, the ions penetrate to achieve osmotic pressure equilibrium inside and outside SAP particles when SAP was placed in deionized water for 70 d. And it was reported that pH value and ion concentration of the solvent change after SAP swelling [31,49]. Therefore, long-term exposure to deionized water can also result in aging phenomena, such as reducing ion concentration in SAP, thus leading to a lower re-swelling ratio compared to that of raw SAP.

However, as shown in Fig. 4, the swelling ratio of the A-CPS group in deionized water is 227.6 g/g and 26.7 % higher than that of the raw SAP. This was because the CPS destroyed the SAP molecule structure, leading to the potential loss of ester groups. This resulted in a reduced crosslinking degree and an increase in the crosslinking network aperture. The lower the crosslinking degree, the higher the water absorption ratio [30,31]. Thus, the A-CPS group exhibits a higher swelling ratio in deionized water and tap water than raw SAP and A-DW group. However, the swelling ratio of the A-CPS group in saturated  $\text{Ca}(\text{OH})_2$  solution is 50.3 % lower than that of the raw SAP, indicating that additional uptake of the electrolyte solution was blocked. The structure of the SAP molecules was destroyed by the alkaline solution environment, thereby the swelling ratio decreased significantly with the increase in ion concentration. The above results indicate that the aging of SAP also occurred in CPS, leading to a reduction in its swelling properties, and the morphology of raw SAP and A-CPS are shown in Fig. S1 and Fig. S2, respectively.

### 3.2.2. Particle size of the SAP aged in solution

To further investigate whether aged SAP splits and whether the size of its degraded fragments poses a potential risk for microplastic pollution, we analyzed the particle size distribution of aged SAP, and the result is presented in Fig. 5. As shown in Fig. 5A, most of the particles of raw SAP have a size around 100–300  $\mu\text{m}$ , while in the A-DW and A-CPS groups, it is primarily around 10–200  $\mu\text{m}$ . The particle size of aged SAP in both DW and CPS shifted towards smaller particles, while a new peak emerged around 0.1–10  $\mu\text{m}$ . Fig. 5B shows that the mean and median particle size of raw SAP are 154.46 and 145.84  $\mu\text{m}$ , respectively. Compared to the raw SAP, these values of the A-DW group are reduced by 40.8 % and 41.2 %, respectively, while in the A-CPS group, they are reduced by 38.3 % and 48.0 %, respectively. It indicates that the structure of SAP particles was destroyed during the aging process, and some of the SAP particles were split into smaller fragments. The particle size of the aged product has partially decreased to around 0.1–200  $\mu\text{m}$ , and it contains a significant number of fragments with particle sizes smaller than 1.0  $\mu\text{m}$ , which may contribute to nano-microplastic pollution. If these fragments migrate into the surrounding environment, they pose a potential risk for microplastic pollution as the service life of the concrete structure extends.

### 3.2.3. TG of the SAP aged in solution

The process of thermal decomposition in polymers is closely related to their molecular structure. To further investigate the

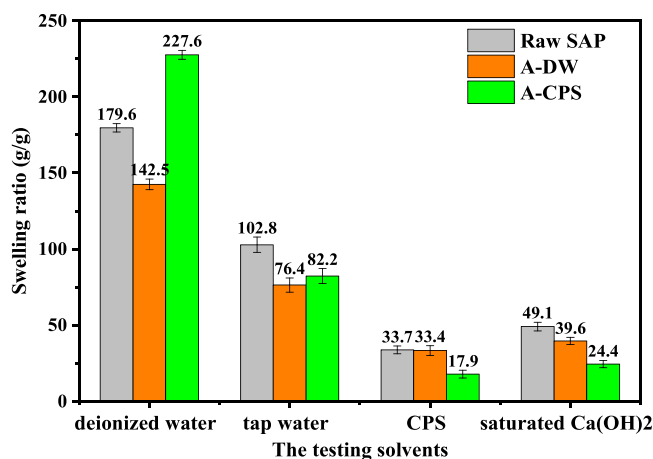


Fig. 4. Swelling property of SAP.

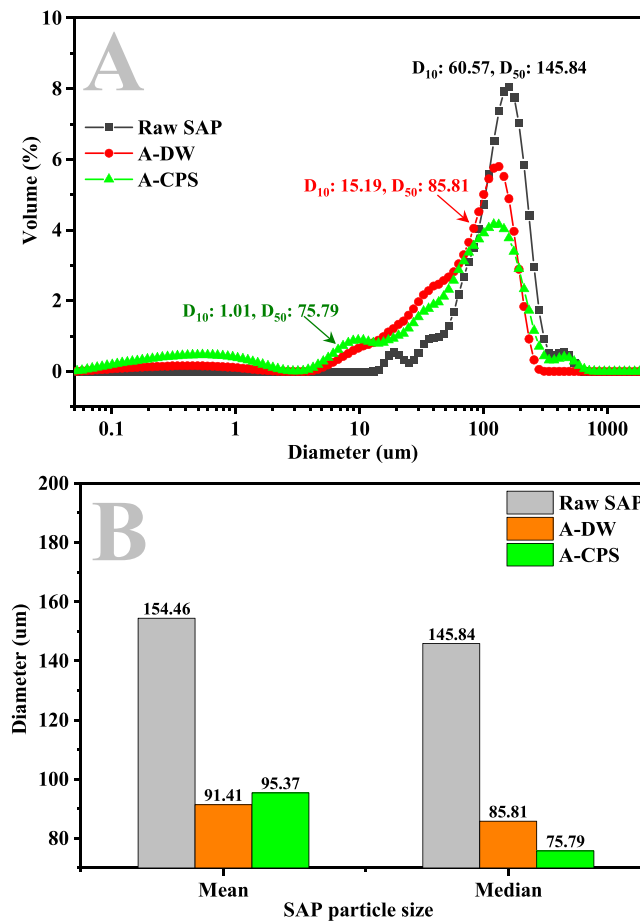


Fig. 5. Particle size distribution of SAP (A: Particle size distribution, B: Mean and median particle size).

mechanisms behind the changes in swelling properties and particle size, TG was conducted to examine the evolution of the molecular structure of SAP before and after aging. The TG curve of the raw SAP in Fig. 6 exhibits four distinct temperature regions with mass loss. The region below 150 °C is associated with the loss of free water and bound water [49]. The region between 265–540 °C indicates that SAP begins to partially decompose, probably related to the breakage of the crosslinked ester group (265–410 °C) and the side chains (410–540 °C) [31,49]. Mass loss observed after 640 °C is related to the breakdown of the backbone chain, indicating that SAP is essentially fully decomposed.

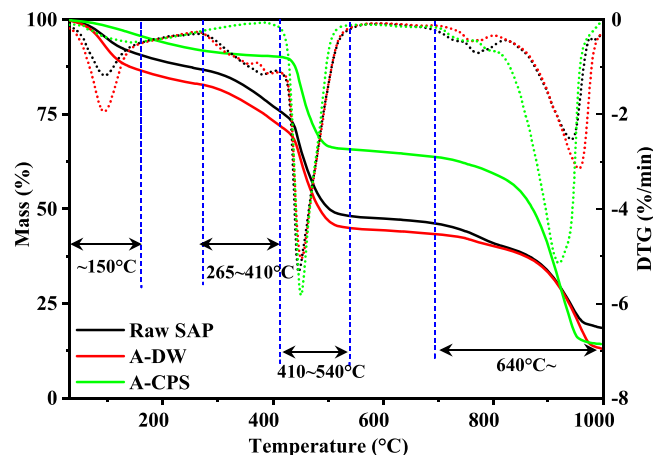


Fig. 6. TG curve of SAP.

The TG curves of the A-DW group and raw SAP are nearly identical, but the A-DW group contains more free water and bound water than the raw SAP. This finding is consistent with the swelling property results. In contrast to the raw SAP, the A-CPS group exhibited a significant reduction in the mass loss region before 150 °C and between 265–410 °C. It implies less free water and bound water in the A-CPS group, and the ester groups have almost disappeared after being aged in CPS for 70 d [31,49]. Furthermore, the enhanced mass loss observed after 640 °C, along with the shift of the decomposition temperature towards lower values, indicates that the backbone chain in the A-CPS group is more prone to breakage. More significantly, these results imply a reduced crosslinking degree of SAP after aging in the CPS, which can explain the change in its swelling property effectively.

### 3.2.4. IR spectra of the SAP aged in solution

To further explore the molecular structure change of SAP in a cement pore solution environment, the IR spectra of raw SAP, the A-CPS group, and the A-DW group were tested, and the results are shown in Fig. 7A. Compared to the raw SAP, the IR spectrum of the A-DW group in Fig. 7A shows a slightly different curve. The peak of the O–H bond around 3590  $\text{cm}^{-1}$  [31,50] moves towards shorter wavelengths, indicating more free water and bound water in the A-DW group are generated compared to the raw SAP. The intensity of peaks at 1720  $\text{cm}^{-1}$  and 1115  $\text{cm}^{-1}$  attributed to the  $-\text{COOC}-$  [29,43] has been reduced. Meanwhile, the peaks attributed to  $-\text{COO}^-$  group at 1573  $\text{cm}^{-1}$  and 1408  $\text{cm}^{-1}$  [31,44,45] are significantly enhanced. Combined with the reduced ester group, it is concluded that the  $-\text{COOC}-$  was hydrolyzed to form  $-\text{COO}^-$  group. This result indicates that some ester groups in the SAP aged in deionized water for 70 d were hydrolyzed into carboxyl groups.

Fig. 7A also shows that the IR spectrum of the A-CPS group is significantly different from that of raw SAP. The peak position of the O–H bond [31] shifts to around 3415  $\text{cm}^{-1}$  and the peak intensity is intensified. The peaks at 1720  $\text{cm}^{-1}$  and 1115  $\text{cm}^{-1}$  attributed to the  $-\text{COOC}-$  group [29,43] almost disappeared. Meanwhile, the peaks at 1573  $\text{cm}^{-1}$  and 1408  $\text{cm}^{-1}$ , which are attributed to the  $-\text{COO}^-$  group [31,44,45] are increased and shifted from 1408  $\text{cm}^{-1}$  to around 1425  $\text{cm}^{-1}$ , indicating an increment in the amount of carboxyl groups in the A-CPS group. Furthermore, the intensity of peak at 870  $\text{cm}^{-1}$  related to unsaturated olefins ( $-\text{CH}=\text{CH}_2-$ ) in SAP [46] increases and the position shifts to around 890  $\text{cm}^{-1}$ , indicating the generation of more  $-\text{CH}=\text{CH}_2-$  bonds. This result indicates that the  $-\text{COOC}-$  group of SAP aged in CPS for 70 d was hydrolyzed to form large amounts of  $-\text{COO}^-$  groups, and the amount of  $-\text{CH}=\text{CH}_2-$  in

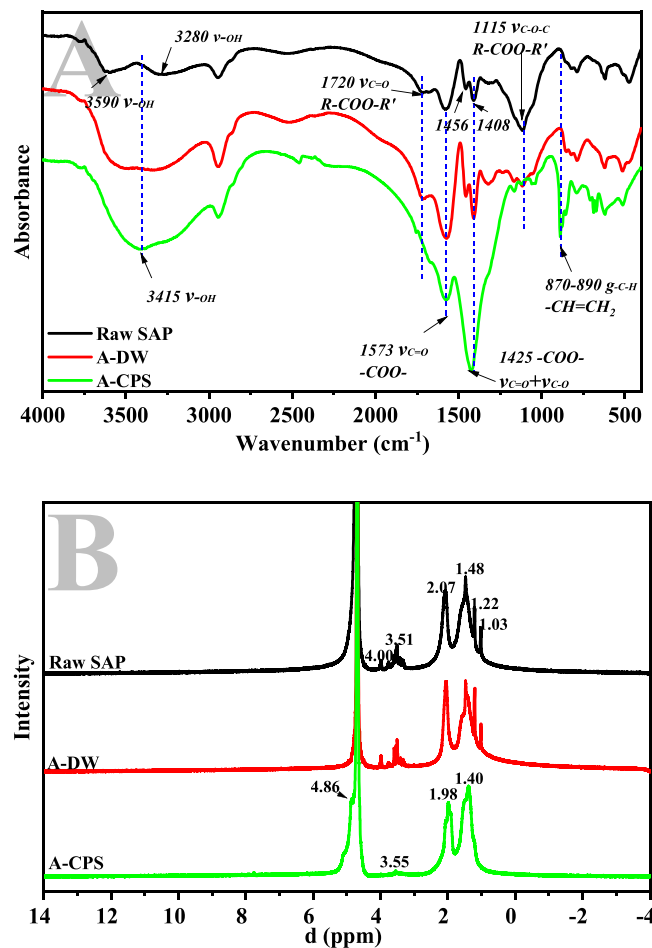


Fig. 7. IR and  $^1\text{H}$  NMR spectra of aged SAP.

the molecule increased. This finding is consistent with the TG results shown in Fig. 6.

### 3.2.5. $^1\text{H}$ NMR spectra of the SAP aged in solution

The  $^1\text{H}$  NMR spectra of raw SAP, A-CPS group, and A-DW group were analyzed to evaluate the changes in molecular structure due to aging, and the results are presented in Fig. 7B. It shows that the  $^1\text{H}$  NMR spectrum of the A-DW group is very similar to that of the raw SAP, but the A-CPS group is significantly altered. Multiple peaks emerge in the region around 1.03–1.48 ppm and shift to 1.40 ppm. The re-aggregation of various molecular weight polymers in the raw SAP in an alkaline solvent is likely the cause of this change [47,48]. Meanwhile, the peak shifting from 2.07 ppm to 1.98 ppm implies an increase in the carboxylate content [47,48]. The multiple peaks associated with the  $-\text{CH}-$  in the alcohol group around 3.51–3.40 ppm appear at 3.55 ppm [29] and the intensity are significantly reduced. This further demonstrates that the multimolecular weight polymer of raw SAP was re-polymerized in an alkaline solvent environment. Furthermore, the new peak appearing at 4.86 ppm may be related to the end alcohol group ( $-\text{O}-\text{H}$ ) [29], indicating that A-CPS group may contain a certain amount of end alcohol groups. These results suggest that the molecular structure of SAP was slightly affected after aging in deionized water but significantly altered in CPS. The findings in  $^1\text{H}$  NMR analysis are also consistent with those from TG and IR curves.

### 3.3. General discussion of aging behavior of SAP in cement-based materials

SAP can store a significant amount of water in its network structure and gradually release the absorbed water to mitigate autogenous shrinkage as an internal curing agent in cement-based materials [23,25,51]. However, the results above indicate that SAP was ultimately aged in cement-based materials after 70 d. This aging behavior is significantly influenced by  $\text{Ca}^{2+}$  concentration and alkalinity of the solution.

In the deionized water, the  $\text{Ca}^{2+}$  concentration is low, approaching 0 mol/L. SAP allows the external deionized water to permeate the polymer until the osmotic pressure—generated by the concentration of ions both inside and outside the polymer—reaches equilibrium, as shown in Fig. 1B. This process is illustrated in Fig. 8. When cations migrate from the SAP to deionized water, the aging products in the deionized water exhibit a molecular structure similar to that of the raw SAP.

In the CPS with a  $\text{Ca}^{2+}$  concentration of 0.01 mol/L, SAP will form three-dimensional networks that absorb a significant amount of water and ionize  $-\text{COO}^-$  groups and  $\text{Na}^+$  upon contact with the solution [28–30], as illustrated in Fig. 8A. Then, the external  $\text{Na}^+$  and  $\text{K}^+$  ions in the CPS solution enter the polymer until the osmotic pressure generated by the concentration of ions inside and outside the polymer reaches equilibrium. Subsequently, these  $-\text{COO}^-$  groups react with  $\text{Na}^+$  and  $\text{K}^+$  ions to form new types of carboxylates. Meanwhile, the  $-\text{COOC}-$  groups are hydrolyzed in an alkaline solution, leading to the generation of  $-\text{COO}^-$  and  $-\text{OH}$  groups, as shown in Eq. 2. Thus, the ester group of SAP nearly disappeared in the CPS, resulting in a significant reduction in the cross-linking degree. The water absorption capacity of SAP is related to the concentration of hydrophilic ions and the crosslinking structure [30,31]. This change

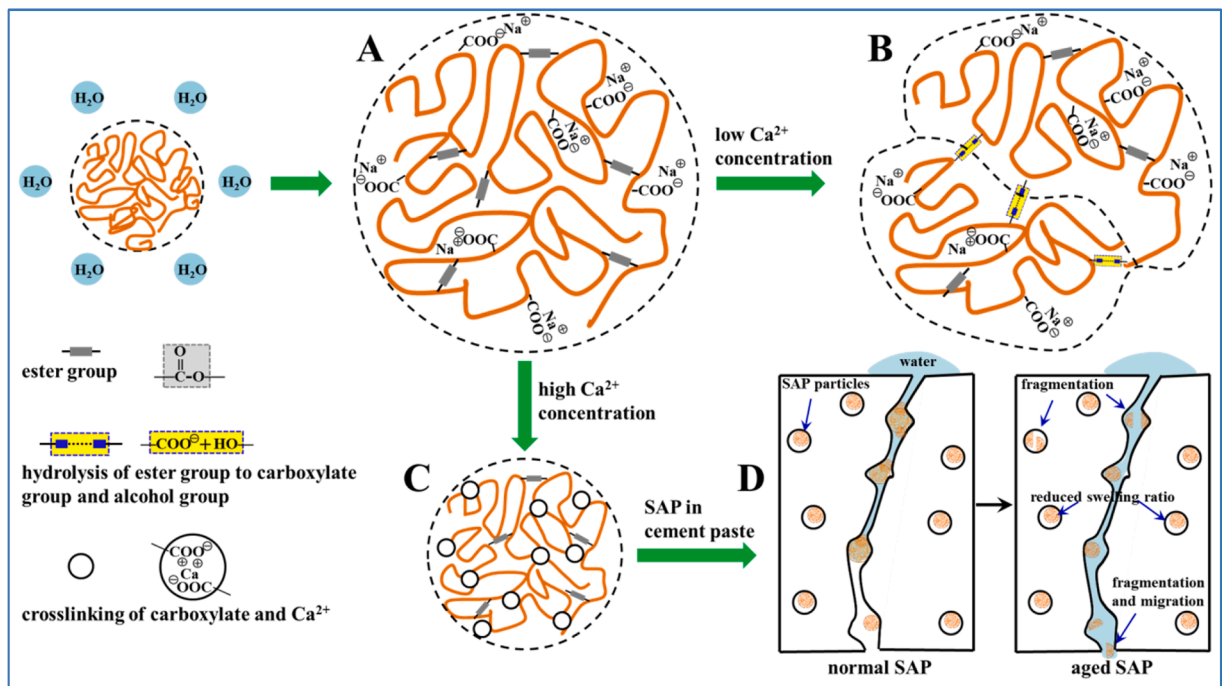
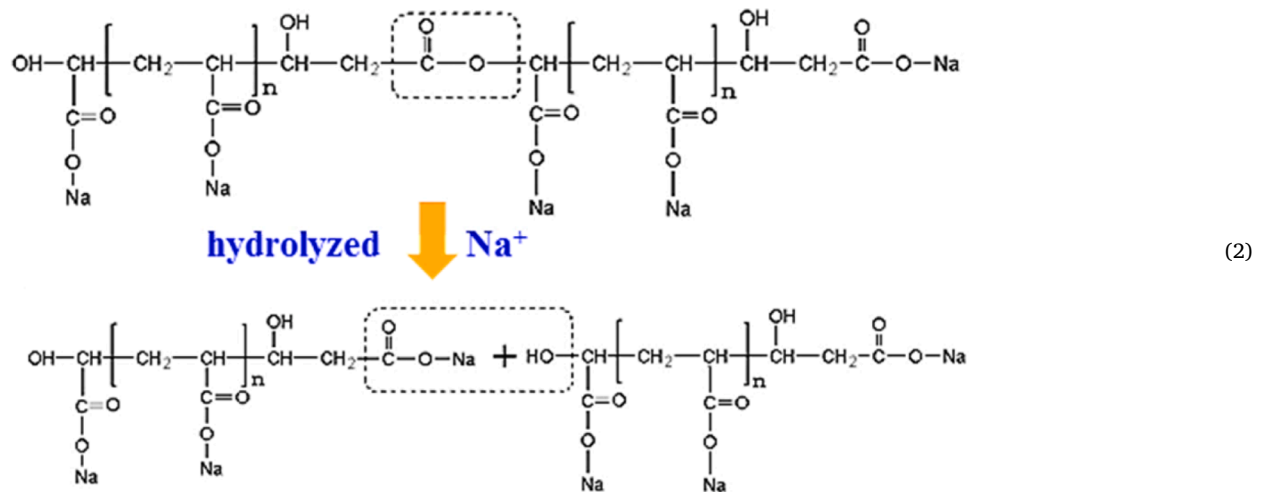


Fig. 8. Aging behavior of SAP (A: SAP swells after absorbing water; B: SAP hydrolysis in the environment with low  $\text{Ca}^{2+}$  concentration; C: SAP crosslinked in the environment with high  $\text{Ca}^{2+}$  concentration; D: Aging and fragmentation of SAP particles in cement paste).

led to an increased swelling ratio of aged SAP in deionized water but a decreased ratio in an electrolyte solution. Additionally, the large SAP particles were fragmented into smaller particles, as depicted in Fig. 8B. The morphology of SAP aging in CPS is provided in Fig. S2.



In cement paste, the pore solution environment contains a higher  $\text{Ca}^{2+}$  concentration compared to that of CPS. These  $\text{Ca}^{2+}$  ions are continuously replenished from the solid phases. The ions in the cement pore solution, such as  $\text{Na}^+$ ,  $\text{K}^+$ , and  $\text{Ca}^{2+}$ , may enter the polymer. Subsequently, part of the  $\text{Ca}^{2+}$  ions crosslink with  $-\text{COO}^-$  groups in SAP particles. Thus, the SAP crosslinks and shrinks in the environment with a high concentration of  $\text{Ca}^{2+}$  ions as these ions are continuously dissolved and replenished during the cement hydration process, as shown in Fig. 8C. Moreover, with the continuous cross-linking of SAP, it becomes challenging for its aged products to absorb water and re-swell. Thus, the SAP hydrolyzes in environments with low  $\text{Ca}^{2+}$  concentration, while it crosslinks in environments with high  $\text{Ca}^{2+}$  concentration.

The results of this work indicate that the SAP ultimately ages in cement-based materials, and the aged SAP may not effectively reabsorb water. The internal curing and self-healing functions provided by SAP rely on their excellent swelling properties [32,33]. Consequently, there are certain concerns about whether SAP can still provide internal curing and self-healing functions in cement-based materials after a certain period, particularly after being hydrated for 70 d. Furthermore, the fragmentation of SAP may migrate outside the system along existing cracks as the service life of the concrete structure prolongs, as illustrated in Fig. 8D. This fragmentation can release microplastic pollution, posing a threat to the safety of the surrounding water environment and potentially impacting human health. This issue is particularly concerning for concrete structures that incorporate SAP, such as water pipes and dams, which come into direct contact with drinking water.

#### 4. Conclusion

In this work, the aging behavior of SAP in cement paste and various solutions for 70 d was studied, and the re-swelling ability of aged SAP and its aging mechanism were analyzed by tests of swelling ratio, particle size distribution, TG, IR, and  $^1\text{H}$  NMR spectrum. The potential microplastic pollution risks posed by the aging products were also evaluated. Based on the experimental results above, the following conclusions are drawn:

- In the range of SAP content less than 1.0 %, the setting times, fluidity, and homogeneity of the cement paste decrease with the increase of SAP content. The SAP particles in cement paste were aged, and its ester groups decreased, carboxylate groups changed, and the aged SAP particles were difficult to re-swell.
- The SAP aged in deionized water for 70 d shows slight aging. Compared with the raw SAP, its swelling ratio is slightly lower, and particle size decreases, with the mean and median particle size values reduced by 40.8 % and 41.2 %, respectively, compared to the raw SAP.
- After aging in CPS for 70 d, the SAP shows significant aging. Compared to the raw SAP, its swelling ratio in CPS decreases by 46.9 %. The original 100–300  $\mu\text{m}$  SAP fragments into 0.1–200  $\mu\text{m}$  particles, with a new 0.1–10  $\mu\text{m}$  peak emerging, making it a potential microplastic pollutant. Moreover, the mean and median particle size values decrease by 38.3 % and 48.0 % respectively, compared to the raw SAP. In terms of particle size, the mean and median values decline by 38.3 % and 48.0 % respectively. Moreover, the molecular structure of the aged SAP changes remarkably: ester groups nearly disappear, while the carboxylate content increases substantially.

The results indicate that the aging of SAP in cement-based materials is inevitable. The aging products cannot reabsorb water and swell as effectively as the raw SAP. As a result, after a certain period, the aged SAP may not be able to perform internal curing functions as the raw SAP. Moreover, the particle size decreases, making it a potential microplastic pollutant, and the cumulative release of these

microplastic pollutants may pose a threat to the surrounding environment. Considering that numerous concrete structures like water pipes and dams are in direct contact with drinking water, SAP should be used cautiously in these water-contact structures, and the potential microplastic pollution release caused by aged SAP deserves further investigation.

### CRedit authorship contribution statement

**Gu Linan:** Writing – review & editing, Writing – original draft, Resources, Project administration, Investigation, Formal analysis, Data curation, Conceptualization. **Feng Jingjing:** Resources, Investigation. **Huang Liming:** Writing – review & editing, Methodology, Investigation, Conceptualization. **Zhu Zheyu:** Writing – review & editing, Resources, Investigation, Conceptualization.

### Declaration of Competing Interest

The authors declare that they have no known competing financial interests or personal relationships that could have appeared to influence the work reported in this paper.

### Acknowledgements

The authors gratefully acknowledge the financial supports provided by the National Natural Science Foundation of China (52302030, 52402031 and 52178227), and the Swedish Research Council (VR, NO. 2024-00569)

### Appendix A. Supporting information

Supplementary data associated with this article can be found in the online version at [doi:10.1016/j.cscm.2025.e04441](https://doi.org/10.1016/j.cscm.2025.e04441).

### Data Availability

The data that has been used is confidential.

### References

- [1] D. Yang, H. Shi, L. Li, J. Li, K. Jabeen, P. Kolandhasamy, Microplastic pollution in table salts from China, *Environ. Sci. Technol.* 49 (22) (2015) 13622–13627.
- [2] B. Xue, L. Zhang, R. Li, Y. Wang, J. Guo, K. Yu, S. Wang, Underestimated microplastic pollution derived from fishery activities and "hidden" in deep sediment, *Environ. Sci. Technol.* 54 (4) (2020) 2210–2217.
- [3] A. Markic, J.H. Bridson, P. Morton, L. Hersey, T. Maes, M. Bowen, Microplastic pollution in the surface waters of Vava'u, Tonga, *Mar. Pollut. Bull.* 185 (2022) 114243.
- [4] S.M. Ladewig, G. Coco, J.A. Hope, A.M. Vieillard, S.F. Thrush, Real-world impacts of microplastic pollution on seafloor ecosystem function, *Sci. Total Environ.* 858 (2023) 160114.
- [5] T. Islam, Y. Li, M.M. Rob, H. Cheng, Microplastic pollution in Bangladesh: Research and management needs, *Environ. Pollut.* 308 (2022) 119697.
- [6] J.O. Jimoh, S. Rahmah, S. Mazelan, M. Jalilah, J.B. Olanunmi, L.S. Lim, M.A. Ghaffar, Y.M. Chang, K. Bhubalan, H.J. Liew, Impact of face mask microplastics pollution on the aquatic environment and aquaculture organisms, *Environ. Pollut.* 317 (2023) 120769.
- [7] Y. Zhou, V. Ashokkumar, A. Amobonye, G. Bhattacharjee, R. Sirohi, V. Singh, G. Flora, V. Kumar, S. Pillai, Z. Zhang, M.K. Awasthi, Current research trends on cosmetic microplastic pollution and its impacts on the ecosystem: A review, *Environ. Pollut.* 320 (2023) 121106.
- [8] N. Koutsikos, A.M. Koi, C. Zeri, C. Tsangaris, E. Dimitriou, O.I. Kalantzi, Exploring microplastic pollution in a Mediterranean river: The role of introduced species as bioindicators, *Heliyon* 9 (2023) 15069.
- [9] S. Eo, S.H. Hong, Y. Cho, Y.K. Song, G.M. Han, W.J. Shim, Spatial distribution and historical trend of microplastic pollution in sediments from enclosed bays of South Korea, *Mar. Pollut. Bull.* 193 (2023) 115121.
- [10] L. Huang, S. Zhang, L. Li, S. Zhang, J. Wang, X. Liu, W. Zhang, Research progress on microplastics pollution in polar oceans, *Polar Sci.* 36 (2023).
- [11] P. Zhang, Y. Yuan, J. Zhang, T. Wen, H. Wang, C. Qu, W. Tan, B. Xi, K. Hui, J. Tang, Specific response of soil properties to microplastics pollution: A review, *Environ. Res.* 232 (2023) 116427.
- [12] D. Briassoulis, Agricultural plastics as a potential threat to food security, health, and environment through soil pollution by microplastics: Problem definition, *Sci. Total Environ.* 892 (2023) 164533.
- [13] Y. Sun, C. Duan, N. Cao, X. Li, X. Li, Y. Chen, Y. Huang, J. Wang, Effects of microplastics on soil microbiome: The impacts of polymer type, shape, and concentration, *Sci. Total Environ.* 806 (2022) 150516.
- [14] N. Nawar, M.M. Rahman, F.N. Chowdhury, S. Marzia, M.M. Ali, M.A. Akbor, M.A.B. Siddique, M.A. Khatun, M. Shahjalal, R. Huque, G. Malafaia, Characterization of microplastic pollution in the Pasur river of the Sundarbans ecosystem (Bangladesh) with emphasis on water, sediments, and fish, *Sci. Total Environ.* 868 (2023) 161704.
- [15] H. Wu, J. Hou, X. Wang, A review of microplastic pollution in aquaculture: Sources, effects, removal strategies and prospects, *Ecotoxicol. Environ. Saf.* 252 (2023) 114567.
- [16] J. Palmer, S. Herat, Ecotoxicity of Microplastic Pollutants to Marine Organisms: a Systematic Review, *Water, Air, Soil Pollut.* 232 (2021) 195.
- [17] M. Smith, D.C. Love, C.M. Rochman, R.A. Neff, Microplastics in Seafood and the Implications for Human Health, *Curr. Environ. Health Rep.* 5 (2018) 375–386.
- [18] T. Wang, L. Qu, D. Luo, X. Ji, Z. Ma, Z. Wang, R.A. Dahlgren, M. Zhang, X. Shang, Microplastic pollution characteristics and its future perspectives in the Tibetan Plateau, *J. Hazard Mater.* 457 (2023) 131711.
- [19] E. Brown, A. MacDonald, S. Allen, D. Allen, The potential for a plastic recycling facility to release microplastic pollution and possible filtration remediation effectiveness, *J. Hazard Mater. Adv.* 10 (2023) 100309.
- [20] S. Sharma, S. Chatterjee, Microplastic pollution, a threat to marine ecosystem and human health: a short review, *Environ. Sci. Pollut. Res. Int.* 24 (2017) 21530–21547.

- [21] A.I. Osman, M. Hosny, A.S. Eltaweil, S. Omar, A.M. Elgarahy, M. Farghali, P.-S. Yap, Y.-S. Wu, S. Nagandran, K. Batumalaie, S.C.B. Gopinath, O.D. John, M. Sekar, T. Saikia, P. Karunanithi, M.H.M. Hatta, K.A. Akinyede, Microplastic sources, formation, toxicity and remediation: a review, *Environ. Chem. Lett.* 21 (2023) 2129–2169.
- [22] H.A. Leslie, M.J.M. van Velzen, S.H. Brandsma, A.D. Vethaak, J.J. Garcia-Vallejo, M.H. Lamoree, Discovery and quantification of plastic particle pollution in human blood, *Environ. Int.* 163 (2022) 107199.
- [23] F. Chen, S. Bai, X. Guan, J. Qiao, H. Gou, Influence of type and particle size of superabsorbent polymer on early water distribution and internal curing zone properties of cement paste, *Cem. Concr. Compos.* 150 (2024) 105526.
- [24] S.-H. Kang, S.-G. Hong, J. Moon, Absorption kinetics of superabsorbent polymers (SAP) in various cement-based solutions, *Cem. Concr. Res.* 97 (2017) 73–83.
- [25] D. Snoeck, L.F. Velasco, A. Mignon, S. Van Vlierberghe, P. Dubruel, P. Lodewyckx, N. De Belie, The effects of superabsorbent polymers on the microstructure of cementitious materials studied by means of sorption experiments, *Cem. Concr. Res.* 77 (2015) 26–35.
- [26] A. Bahari, A. Sadeghi-Nik, M. Roodbari, A. Sadeghi-Nik, E. Mirshafiei, Experimental and theoretical studies of ordinary Portland cement composites contains nano LSCO perovskite with Fokker-Planck and chemical reaction equations, *Constr. Build. Mater.* 163 (2018) 247–255.
- [27] A. Bahari, A. Sadeghi-Nik, F.A. Shaikh, A. Sadeghi-Nik, E. Cerro-Prada, E. Mirshafiei, M. Roodbari, Experimental studies on rheological, mechanical, and microstructure properties of self-compacting concrete containing perovskite nanomaterial, *Struct. Concr.* 23 (2022) 564–578.
- [28] F. Ai, X. Yin, R. Hu, H. Ma, W. Liu, Research into the super-absorbent polymers on agricultural water, *Agr. Water Manag.* 245 (2021) 106513.
- [29] H.J. Kim, J.M. Koo, S.H. Kim, S.Y. Hwang, S.S. Im, Synthesis of super absorbent polymer using citric acid as a bio-based monomer, *Polym. Degrad. Stab.* 144 (2017) 128–136.
- [30] R.A. Rather, M.A. Bhat, A.H. Shalla, An insight into synthetic and physiological aspects of superabsorbent hydrogels based on carbohydrate type polymers for various applications: A review, *Carbohydr Polym. Tech. Appl.* 3 (2022) 100202.
- [31] T.T. Hong, H. Okabe, Y. Hidaka, K. Hara, Radiation synthesis and characterization of super-absorbing hydrogel from natural polymers and vinyl monomer, *Environ. Pollut.* 242 (2018) 1458–1466.
- [32] G. Hong, S. Choi, Rapid self-sealing of cracks in cementitious materials incorporating superabsorbent polymers, *Constr. Build. Mater.* 143 (2017) 366–375.
- [33] H. Liu, Y. Bu, J.G. Sanjayan, A. Nazari, Z. Shen, The application of coated superabsorbent polymer in well cement for plugging the microcrack, *Constr. Build. Mater.* 104 (2016) 72–84.
- [34] I. Rosero, E. Somarriba, B. Farivar, C. Murray, Effects of mixture design parameters on the properties of belitic calcium sulfoaluminate concrete, *Mag. Concr. Res.* 76 (2024) 217–228.
- [35] M. Mousavi, A. Sadeghi-Nik, A. Bahari, A. Ashour, H. Kamal, Cement paste modified by nano-montmorillonite and carbon nanotubes, *Acids Mater. J.* 119 (2022) 173–185.
- [36] GB/T1346-2011, Test methods for water requirement of normal consistency, setting time and soundness of the portland cement (ISO 9597:2008, cement-test methods-determination of setting time and soundness, NEQ) [S], Standardization Administration of China, Beijing, 2011.
- [37] GB/T8077-2000, Methods for Testing Uniformity of Concrete Admixture, Standardization Administration of China, Beijing, 2000.
- [38] GB175-2020, Common Portland Cement, Standardization Administration of China, Beijing, 2000.
- [39] C. Song, Y.C. Choi, S. Choi, Effect of internal curing by superabsorbent polymers–internal relative humidity and autogenous shrinkage of alkali-activated slag mortars, *Constr. Build. Mater.* 123 (2016) 198–206.
- [40] A. Sadeghi-Nik, J. Berenjian, S. Alimohammadi, O. Lotfi-Omran, A. Sadeghi-Nik, M. Karimaei, The Effect of Recycled Concrete Aggregates and Metakaolin on the Mechanical Properties of Self-Compacting Concrete Containing Nanoparticles, *Iran. J. Sci. Technol., Trans. Civ. Eng.* 43 (2019) 503–515.
- [41] A. Bahari, A. Sadeghi-Nik, E. Cerro-Prada, A. Sadeghi-Nik, M. Roodbari, Y. Zhuge, One-step random-walk process of nanoparticles in cement-based materials, *J. Cent. South Univ.* 28 (2021) 1679–1691.
- [42] A. Sadeghi-Nik, J. Berenjian, A. Bahari, A.S. Safaei, M. Dehestani, Modification of microstructure and mechanical properties of cement by nanoparticles through a sustainable development approach, *Constr. Build. Mater.* 155 (2017) 880–891.
- [43] Y. Liao, H. Zheng, L. Qian, Y. Sun, L. Dai, W. Xue, UV-Initiated polymerization of hydrophobically associating cationic polyacrylamide modified by a surface-active monomer: a comparative study of synthesis, characterization, and sludge dewatering performance, *Ind. Eng. Chem. Res.* 53 (2014) 11193–11203.
- [44] M. Jeldres, P. Robles, P.G. Toledo, M. Saldaña, L. Quezada, R.I. Jeldres, Improved dispersion of clay-rich tailings in seawater using sodium polyacrylate, *Colloids Surf. A* 612 (2021) 126015.
- [45] D. Wang, X. Liu, G. Zeng, J. Zhao, Y. Liu, Q. Wang, F. Chen, X. Li, Q. Yang, Understanding the impact of cationic polyacrylamide on anaerobic digestion of waste activated sludge, *Water Res.* 130 (2018) 281–290.
- [46] W.E. Richter, L.J. Duarte, R.E. Bruns, Atomic charge and atomic dipole modeling of gas-phase infrared intensities of fundamental bands for out-of-plane CH and CF bending vibrations, *Spectrochim. Acta A* 251 (2021) 119393.
- [47] W. Kang, X. Hou, C. Chen, S. Shao, X. Zhang, T. Zhu, T. Wang, H. Yang, Study on rheological behavior and salt-thickening mechanism of a synthesized twin-tailed hydrophobically modified polyacrylamide, *J. Mol. Liq.* 294 (2019) 111619.
- [48] N. Shi, D. Zhang, Inorganic-organic composite solid electrolyte based on cement and Polyacrylamide prepared by a synchronous reaction method, *Electro Acta* 391 (2021) 138998.
- [49] S. Fang, G. Wang, R. Xing, X. Chen, S. Liu, Y. Qin, K. Li, X. Wang, R. Li, P. Li, Synthesis of superabsorbent polymers based on chitosan derivative graft acrylic acid-co-acrylamide and its property testing, *Int J. Biol. Macromol.* 132 (2019) 575–584.
- [50] M.A. Kafi, A. Sadeghi-Nik, A. Bahari, A. Sadeghi-Nik, E. Mirshafiei, Microstructural characterization and mechanical properties of cementitious mortar containing montmorillonite nanoparticles, *J. Mater. Civ. Eng.* 28 (2016) 04016155.
- [51] D. Snoeck, O.M. Jensen, N. De Belie, The influence of superabsorbent polymers on the autogenous shrinkage properties of cement pastes with supplementary cementitious materials, *Cem. Concr. Res.* 74 (2015) 59–67.